OXFORD

Social Cognitive and Affective Neuroscience, 2025, **20**(1), nsaf019

DOI: https://doi.org/10.1093/scan/nsaf019
Advance Access Publication Date: 15 February 2025
Original Research – Neuroscience

Crus control: effective cerebello-cerebral connectivity during social action prediction using dynamic causal modelling

Naem Haihambo[1,2,3,*], Kris Baetens[1], Natacha Deroost[1], Chris Baeken[1,4,5], Frank Van Overwalle[1]

[1]Department of Psychology and Center for Neuroscience, Vrije Universiteit Brussel, Brussels 1050, Belgium
[2]Department of Social Neuroscience, Faculty of Medicine, Ruhr University Bochum, Bochum 44801, Germany
[3]Research Center One Health Ruhr of the University Alliance Ruhr, Ruhr University Bochum 44801, Germany
[4]Department of Psychiatry, University Hospital (UZBrussel), Brussels 1090, Belgium
[5]Department of Head and Skin (UZGent), Ghent Experimental Psychiatry (GHEP) Lab, Ghent University, Ghent 9000, Belgium
[*]Corresponding author. Department of Psychology, Vrije Universiteit Brussel, Pleinlaan 2, Brussels B – 1050, Belgium. E-mail: naem.patemoshela.haihambo@vub.be

Abstract

This dynamic causal modeling (DCM) analysis, comprising 99 participants from 4 studies, investigated effective neuronal connectivity during social action sequence prediction. The analysis focused on mentalizing areas within the cerebellum, specifically the bilateral Crus 1, Crus 2, and lobule IX, as well as cerebral mentalizing areas within the precuneus, temporo-parietal junction (TPJ), and dorsal medial prefrontal cortex (dmPFC). Consistent with previous research, we found robust bidirectional closed loop connections between the posterior cerebellar Crus and cerebral mentalizing areas. We also found previously unexplored unidirectional connections originating from cerebellar lobule IX to the dmPFC and left TPJ and from the right TPJ to lobule IX. Furthermore, we uncovered many bidirectional closed loops within the cerebellum between the left and right Crus 1, and between Crus 1 and Crus 2, and for the first time, between the bilateral Crus 2 and lobule IX. Our findings illuminate the distinct role of cerebellar Crus and lobule IX, and cerebral mentalizing areas in predicting social action sequences.

Keywords: dynamic causal modelling (DCM); connectivity; social interactions; posterior cerebellum; social action prediction; social action sequencing; lobule IX

Introduction

The cerebellum has long been recognized as playing a crucial role in motor coordination and balance. However, recent research has demonstrated that this brain region also plays a critical role in a variety of nonmotor functions (Ito 2008), including social mentalizing (Van Overwalle et al. 2014, 2015). Mentalizing refers to our ability to interpret the mental states of others, such as their intentions, preferences, and traits (Molenberghs et al. 2016). Studies have identified key areas involved in mentalizing in the posterior cerebellum, such the Crus 1 and 2 (Van Overwalle et al. 2014), as well as in the cerebrum, such as the temporoparietal junction (TPJ), precuneus, and medial prefrontal cortex (mPFC; Van Overwalle 2009, Schurz et al. 2014, Molenberghs et al. 2016).

Various brain regions appear to play distinct roles in mentalizing. For instance, in the cerebrum, the TPJ is thought to be involved in social perspective switching and inferring other people's current mental states from their actions, the precuneus is involved in mental imagery about social scenes that form the background of people's social actions, and the mPFC is responsible for inferring stable personality traits inferred from social actions (Van Overwalle 2009, Schurz et al. 2014). Meanwhile, the posterior cerebellar Crus areas are thought to be responsible for identifying and automatizing the temporal sequences of actions requiring mentalizing (Leggio and Molinari 2015), including lower-level social inferences, such as intention prediction (Haihambo et al. 2022) and goal-directed spatial navigation (Li et al. 2021, 2023) as well as higher-level inferences such as social beliefs (Heleven et al. 2019, Ma et al. 2021a, 2021b), trait prediction (Haihambo et al. 2022), and trait attribution (Pu et al. 2020).

The cerebellum in mentalizing and social prediction

It has been suggested that the cerebellum's role in social sequencing is a result of its broader sequencing function. According to this "sequencing hypothesis," the cerebellum's core function is

Received: 24 October 2023; Revised: 30 January 2025; Accepted: 13 February 2025

to generate internal models of the temporal sequences involved in motor and nonmotor processes which, over time, allow the automation, anticipation, and smooth execution of these sequences (Ito 2008, Pisotta and Molinari 2014, Leggio and Molinari 2015, Guell et al. 2018). More recently, Van Overwalle et al. (2019a) posited that the cerebellum also supports social mentalizing by facilitating the learning, automation, and anticipation of social action sequences, thereby assisting mentalizing and promoting smooth human interaction and predicting future social (inter)actions of both self and others (Blakemore et al. 2001, Frith and Frith 2006, Sokolov et al. 2017).

Within the cerebellum, the evolutionarily younger posterior areas Crus 1 and 2, and lobule IX have been delineated as being specifically involved in mentalizing in both resting state studies involving mind wandering, often about self-relevant social processes (Buckner et al. 2011) and in meta-analyses that investigated social mentalizing (Van Overwalle et al. 2014, 2015). More recently, a meta-analysis by Van Overwalle et al. (2020a) provided compelling evidence that cerebellar Crus 2 is highly specialized in domain-specific social mentalizing and self-related affective cognition. The cerebellar lobule IX has been implicated in future-oriented thinking, which involves mentalizing about a past and a future self and others (Addis et al. 2007, 2009).

Effective connectivity between the cerebellar and cerebral mentalizing areas

Despite the increasing interest in the role of the cerebellum in social processes, research on the connectivity within and between cerebellar and cerebral mentalizing areas during these processes is still in its early stages. Nonetheless, some studies have demonstrated that the posterior cerebellum is connected to cerebral mentalizing areas. For example, using psychophysiological interaction (PPI) analysis, Metoki et al. (2022) found that mentalizing areas in the cerebellum and cerebrum are strongly functionally connected during mentalizing. Using more robust and biologically plausible functional connectivity methods such as dynamic causal modeling (DCM), studies on social mentalizing found strong evidence for bidirectional effective closed loops (i.e. connections that initiate and terminate in the same cerebellar and cerebral areas) between the bilateral posterior cerebellar Crus 1, Crus 2, and bilateral TPJ, precuneus and mPFC when people inferred others' traits (Van Overwalle et al. 2019b), and during the comprehension of stories involving other's beliefs (Van Overwalle et al. 2020b). These results were further supported and extended in more recent studies. Pu et al. (2022b) investigated the effective connectivity between the cerebellum and cerebrum during trait/stereotype attribution and found significant closed loops between Crus 2 and cerebral mentalizing areas in the TPJ, precuneus, and mPFC. Similarly, during social belief sequence learning, Ma et al. (2023a) found significant bidirectional closed loops between cerebellar Crus 1 and 2 and cerebral mentalizing areas in the TPJ and precuneus (but not with the mPFC, as belief inferences are mainly associated with the TPJ).

Developed by Friston et al. (2003), DCM allows researchers to examine the strength of connections between different regions of the brain by analyzing patterns of neural activity using fMRI. What sets DCM apart from other approaches, such as PPI, is that it allows to analyze the direction of the connections and determines their "effective" (or true causal) strength by controlling for other indirect connections in the brain, allowing for more accurate and biologically plausible models of neural activity. By using DCM, researchers can better understand how different areas of the brain are working together and influencing each other to produce behavior.

Present study: cerebellar connectivity during social action prediction

The present analysis enhances our understanding of closed loops during mentalizing by addressing a number of limitations of previous DCM studies and exploring novel questions. We extended this scope in two ways. First, we investigate the prediction of future action sequences based on mentalizing inferences, expanding upon earlier DCM studies, which primarily focused on the detection or generation of past social action sequences that required mentalizing. Second, we investigate the role of the inferior posterior cerebellar lobule IX within a mentalizing closed-loop network, a cerebellar area that has been overlooked in earlier DCM studies on mentalizing. Indeed, recent studies on social sequencing have shown that participants predicted future actions based on social information, such as traits (Haihambo et al. 2022, 2023a). These findings demonstrated the critical involvement of not only the posterior cerebellar Crus 1 and 2, but also the cerebellar lobule IX, in addition to well-established cerebral mentalizing areas in the bilateral TPJ, precuneus, and (dorsal) mPFC.

In line with previous DCM studies investigating cerebellar involvement during social sequencing that requires mentalizing, we used DCM to analyze four studies involving social predictions based on traits (Haihambo et al. 2022, Haihambo et al. 2023a), intentions (Haihambo et al. 2022), and preferences (Haihambo et al. 2023b). Like previous DCM analyses (Van Overwalle et al. 2019b, 2020b, Pu et al. 2022b, Ma et al. 2023a), we combined these studies resulting in a large number of participants so that the connectivity estimates are stable (Silchenko et al. 2023). We expect to find significant closed loops between posterior cerebellar regions of interest (ROIs; Crus 1 and 2, and lobule IX) and key cerebral mentalizing ROIs (TPJ, precuneus, mPFC).

Method

Participants

The participants in the four studies ($N = 99$; 37 male) were healthy, right-handed, native Dutch-speaking volunteers. All participants had normal or corrected-to-normal vision and reported no neurological or psychiatric disorders. Informed consent was obtained following the guidelines of the Medical Ethics Committee at Gent University Hospital, where all studies were conducted. Participants were given 20 euros per hour and reimbursed for transportation costs in exchange for their participation.

Included studies

We performed DCM (K. Friston et al. 2015, 2016) on the fMRI data of four existing fMRI studies (Haihambo et al. 2022). These studies were selected because they involved predicting social action sequences and used comparable paradigms. As noted earlier, the predictions were based on *a priori* given mentalizing inferences involving traits (Haihambo et al. 2022, Haihambo et al. 2023a), intentions (Haihambo et al. 2023a), and preferences (Haihambo et al. 2023b). Results in these studies found robust activations in the bilateral Crus 1, bilateral Crus 2, medial lobule IX in the (inferior) posterior cerebellum, and in the bilateral TPJ, precuneus, and dorsal medial prefrontal cortex (dmPFC). Together, the compilation of these four studies allows for strong and robust estimates of the effective connectivity of these areas during social action prediction. For the present DCM analysis, we compared the experimental condition (i.e. Social Sequencing) to its nonsocial control

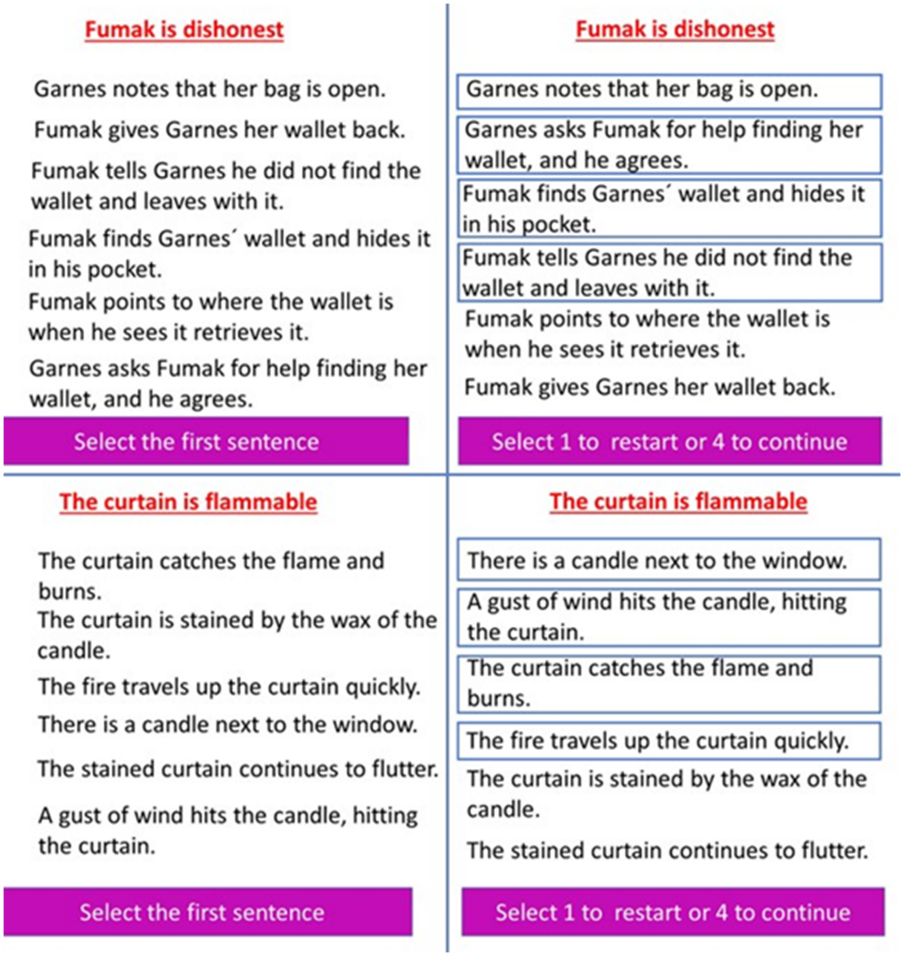

Figure 1. Example of stimulus materials used in Study 1 and 4: illustration of a trial from the Social Sequencing (top panel) and Nonsocial sequencing (bottom panel) conditions. Left panel: participants were presented with six action sentences (randomly ordered) and were required to select the four sentences that best matched the person trait or object feature. They were then instructed to order all four selected sentences one at a time in the correct chronological order, ignoring the trait-inconsistent sentences, using two consecutive button presses on a four-button response box (with responses indicated on a blue background). Right: the ordering as chosen by a participant (the selected four sentences were ordered from top to bottom).

(i.e. Nonsocial Sequencing), because this contrast provided the most consistent activations across all four studies.

The procedure was analogous in all studies. We describe here only the procedural aspects that are included in the DCM analysis, leaving out other conditions that are of no interest here (e.g. Non-sequencing control conditions), and refer to the individual studies for more details. Participants were informed that the experiment included a sequencing task using both Social and Nonsocial stimulus materials. They were further told that they would read information on an agent/object (in the Social/Nonsocial conditions, respectively) at the beginning of each trial, followed by six sentences of which two were neutral, two consistent and two inconsistent with respect to information given one by one in random order. Participants had to select four out of six sentences that logically fit the given prompt sentence (e.g. a trait-related prompt: "Fumak is honest"). Sentences that did not fit the prompt were to be ignored. The prompt sentences appeared in red on the top of the screen, where it remained for the entire duration of the trial. An example of the stimulus materials and the selection procedure is presented in Fig. 1.

In the sequencing task, after 1000 ms, the first of six sentences were shown on the screen followed by the remaining five sentences, which appeared one-by-one after 1300 ms each. Immediately afterwards, all sentences were shown together on screen in the same order along with numbers on the side of the sentences used for responding (Fig. 2). The six sentences were presented in a random order and participants had to select two neutral and two consistent sentences and put them in their correct chronological order. A prompt to select the first sentence appeared at the bottom of the screen, followed by a prompt to select the next sentence, until they selected all sentences. No duration was set for completing this task. Once four sentences were selected, participants were then prompted to select "1 to restart or 4 to continue." Participants responded with a button press using an MRI compatible four button response box positioned in their left hand. All trials were preceded by a blank screen with a fixation cross, jittered randomly between 1 and 2 s.

The only difference between the studies was that they included different social information (i.e. traits, intentions, and preferences) and related scenarios. Specifically, participants were presented with a prompt providing *a priori* information on an agent's trait in Study 1 (e.g. friendly; Haihambo et al. 2022), intentions in Study 2 (e.g. deceitful; Haihambo et al. 2022) and preferences in Study 3 [e.g. wine; (Haihambo et al. 2023a)]. In Study 4,

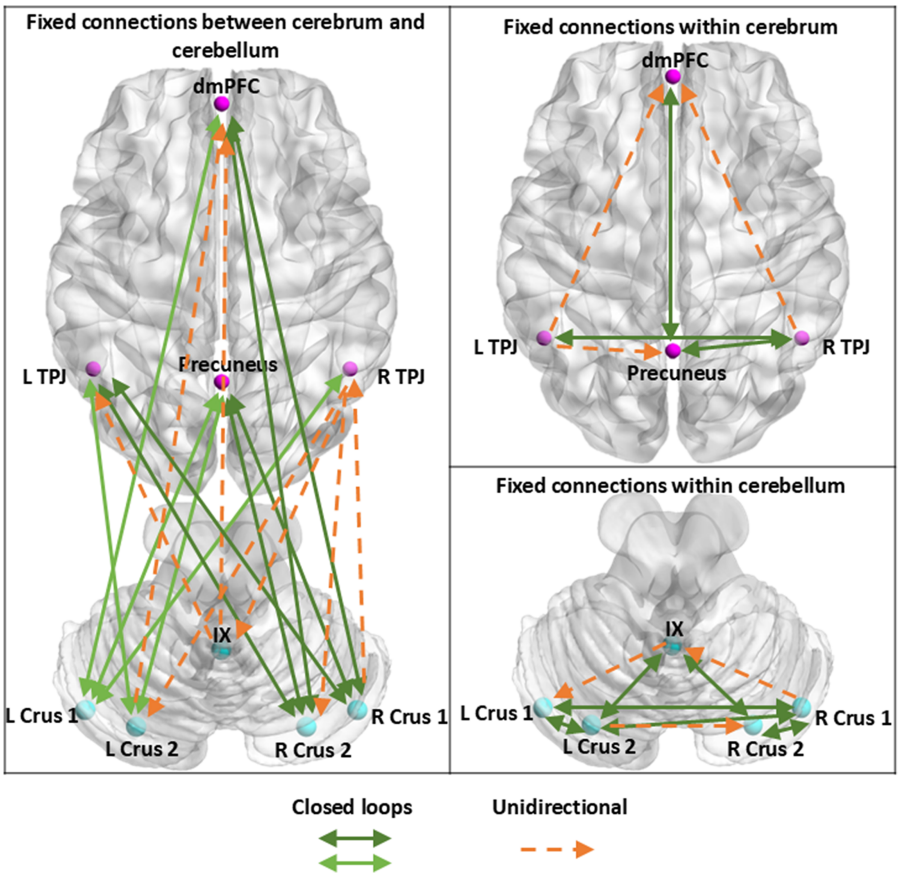

Figure 2. Significant fixed connections in the reduced model of social sequencing, including the cerebellar Crus, lobule IX, precuneus, temporoparietal junction (TPJ), and dorsal medial prefrontal cortex (mPFC) with a posterior probability $P > .95$. Left: connections between the cerebellum and the cerebrum Top right: connections within the cerebrum. Bottom right: connections within the cerebellum. Solid green arrows indicate closed-loop connections, for easier visualization, closed loops with the left cerebellum are in a lighter green shade, while those with the right are darker green. Dashed orange arrows indicate unidirectional connections. The connectivity estimates correspond to rate constants and are expressed in units of 1/s (Hz). Left and right areas are represented on the left and right of the figure, respectively.

participants received the same task as in Study 1, and additionally received anodal cerebellar stimulation before the task (Haihambo et al. 2023a). In this study, participants received 2 mA of anodal stimulation to the midline of the cerebellum, 2 cm below the inion for 20 min, while the reference electrode was placed on the chin.

Imaging procedure and preprocessing

In all studies, images were collected with a Siemens Magnetom Prisma fit scanner system (Siemens Medical Systems, Erlangen, Germany) using a 64-channel radiofrequency head coil. Stimuli were projected onto a screen at the end of the magnet bore, which participants viewed by way of a mirror mounted on the head coil. Participants were placed headfirst and supine in the scanner bore and were instructed not to move their heads to avoid motion artifacts. Foam cushions were placed within the head coil to minimize head movements. First, high-resolution anatomical images were acquired using a T1-weighted 3D MPRAGE sequence [repetition time (TR) = 2250 ms, echo time (TE) = 4.18 ms, inversion time (TI) = 900 ms, field of view (FOV) = 256 mm, flip angle = 9°, voxel size = 1 × 1 × 1 mm]. Second, a fieldmap was calculated to correct for inhomogeneities in the magnetic field (Cusack and Papadakis 2002). Third, whole-brain functional images were collected in a single run using a T2*-weighted gradient echo sequence, sensitive to blood oxygen level dependent (BOLD) contrast [TR = 1000 ms, TE = 31.0 ms, FOV = 210 mm, flip angle = 52°, slice thickness = 2.5 mm, distance factor = 0%, voxel size = 2.5 × 2.5 × 2.5 mm, 56 axial slices, acceleration factor GeneRalized Autocalibrating Partial Parallel Acquisition (GRAPPA) = 4].

SPM12 (Wellcome Department of Cognitive Neurology, London, UK) was used to process and analyze the fMRI data. To remove sources of noise and artifacts, data were preprocessed. Functional data were corrected for differences in acquisition time between slices for each whole-brain volume, realigned to correct for head movement, and co-registered with each participant's anatomical data. Then, the functional data were transformed into a standard anatomical space (2 mm isotropic voxels) based on the ICBM152 brain template (Montreal Neurological Institute). Normalized data were then spatially smoothed (6 mm full width at half-maximum, FWHM) using a Gaussian Kernel. Finally, using the Artifact Detection Tool (ART; http://web.mit.edu/swg/art/art.pdf; http://www.nitrc.org/projects/artifact_detect), the data was examined for excessive motion artifacts and for correlations between motion and experimental design, and between global mean signal and experimental design. Outliers were identified in the temporal differences series by assessing between-scan differences (Z-threshold: 3.0 mm, scan to scan movement threshold: 0.5 mm; rotation threshold: 0.02 radians). These outliers were "omitted" from the analysis by including a single regressor for each outlier. A default high-pass filter was used of 128 s and serial

correlations were accounted for by the default auto-regressive (AR) model.

Dynamic causal modeling

To apply DCM, regions of interest (ROIs) indicating core cerebellar and cerebral mentalizing areas were identified. These regions were the cerebellar Crus 1 and 2 (centered at ±40 −70 −40 and ±24 −76 −40, respectively) from the meta-analysis by Van Overwalle et al. (2020a), and cerebral mentalizing areas including the mPFC (0, 50, 20), bilateral TPJ (±50 −55 25), and precuneus (0 −60 10) from meta-analyses on social cognition (Van Overwalle 2009, Van Overwalle and Baetens 2009). For the novel cerebellar lobule IX, we used the peak coordinates (0 −52 −40) averaged across our previous activation studies (Haihambo et al. 2022, 2023a, 2023b).

Our DCM analysis was based on a contrast that was present in all studies and showed robust cerebellar and cerebral activation in the mentalizing ROIs (i.e. Social Sequencing > Nonsocial Sequencing). The ROI coordinates were used as center for group-based ROIs defined as spheres with a radius of 15 mm for the cerebrum and 10 mm for cerebellum (given the smaller volume). Following the procedure in Van Overwalle et al. (2020b), individually tailored cerebral ROIs were created by extracting time series of this contrast using the eigenvariate within a sphere with a smaller individual radius of 8 mm for the cerebrum and 5 mm for the cerebellum around the nearest local maximum of the corresponding group ROI. This was done after setting the whole-brain threshold at $P < .05$ (uncorrected). If the ROIs did not survive the threshold, the same procedure was repeated with $P < .10$ and $P < 1.00$ (uncorrected) so that the time series of all ROIs were included for all participants (see Table 1 for the number of ROIs that fulfilled these criteria). In the latter case (i.e. $P < 1.00$), ROIs were centered around the group-based centers listed above (Zhou et al. 2007). This procedure is followed because DCM analysis requires time series from all ROIs, making pairwise exclusion impossible. So, setting a more tolerant threshold in some individual cases allows for the effect of interest to be maximized at an individual level, while including all participants in the analysis without introducing a bias from excluding some participants (Zhou et al. 2007).

To estimate the optimal DCM across all participants and studies, we followed the procedures described in Friston et al. 2015, 2016 and given in full detail in https://en.wikibooks.org/wiki/User:Peterz/sandbox.

First, a full DCM was specified and estimated for each participant using SPM12 (cf. the SPM procedure: spm_dcm_fit). A full model allows all connectivity parameters in all directions to be freely estimated. We specified a bilinear deterministic DCM without centering around the mean (Friston et al. 2003), which included (i) fixed connections; all forward and backward fixed connections between the ROIs, (ii) modulatory connections; all the modulatory connections or parameters that reflected condition changes due to the mentalizing condition in particular connections, and (iii) direct input parameters; connections that reflected the input driving the activity in both conditions in the ROIs. Stated differently, the driving input in Matrix C consists of one vector with all the onsets of both the mentalizing and control conditions combined as one input, and the modularity connections in Matrix B are specified only for the mentalizing condition, so that both matrix inputs are nonredundant to each other (Hillebrandt et al. 2014). The order of the conditions in the DCM for all studies was arranged so that the two conditions of interest were aligned (i.e. the critical experimental and control condition specified above for each study). Note that the connections in DCMs

Table 1. ROIs for DCM analysis, total number of participants (N), and number of participants at tolerant thresholds.

	MNI coordinates			Study 1 (trait prediction)			Study 2 (intention prediction)			Study 3 (preference prediction)			Study 4 (trait prediction, anodal cerebellar tDCS)		
				Haihambo et al. (2022)			Haihambo et al. (2023a)			Haihambo et al. (2023b)			Haihambo et al. (2022)		
				$n = 26$			$n = 24$			$n = 27$			$n = 22$		
Region	x	y	z	<0.05	<0.1	<1	<0.05	<0.1	<1	<0.05	<0.1	<1	<0.05	<0.1	<1
Cerebellar ROIs															
L Crus 1				26	0	1	21	0	3	20	2	0	17	3	2
R Crus 1	−40	−70	−40	25	1	1	23	0	1	20	1	1	21	1	0
L Crus 2	−25	−75	−40	26	1	0	24	0	0	22	0	0	21	0	1
R Crus 2	25	−75	−40	26	1	0	24	0	0	21	1	0	21	1	0
Lobule IX	0	−52	−44	27	0	0	23	1	0	21	0	1	22	0	0
Cerebral ROIs															
Precuneus	0	−60	40	27	0	0	24	0	0	22	0	0	22	0	0
L TPJ	−50	55	25	27	0	0	24	0	0	22	0	0	22	0	0
R TPJ	−50	55	25	27	0	0	24	0	0	22	0	0	22	0	0
dmPFC	0	50	35	27	0	0	24	0	0	22	0	0	22	0	0

Note: L = left, R = right, TPJ = temporoparietal junction, mPFC = medial prefrontal cortex.

correspond to rate constants and are expressed in units of 1/s (i.e. of hertz).

Second, we constructed a parametric empirical Bayes (PEB) model for the whole group of participants over all parameters (cf. the SPM procedure: spm_dcm_peb). This makes it possible to estimate the effective connectivity averaged across all participants (cf. the group average), taking into account the within-participants variability on the connectivity parameters, unlike in a classical test (e.g. a *t*-test), which ignores the estimated uncertainty (variance) about the connection strengths. Moreover, a group-level PEB allows controlling differences between sets of studies by treating them as covariates (e.g. differences in the behavioral measures and procedures; (Friston et al. 2016).

In our model, we focused on the common connectivities across all four studies, and at the PEB group-level, we controlled for differences between studies by contrasting the studies against each other (e.g. Study 1 > 2, Study 1 > 3, Study 1 > 4). This approach allowed us to account for any potential confounding effects related to differences in study design, participant characteristics, or other variables that might vary between studies. By including these contrasts as covariates of no interest, we were able to isolate the shared connectivity patterns across all studies while controlling for study-specific effects. Note that contrasting one study against all other studies is sufficient to control for all differences between studies at the PEB group-level.

Third, we automatically pruned away any connectivity parameter from the group-level PEB that did not contribute to the model evidence, using Bayesian model reduction (cf. the SPM procedure: spm_dcm_peb_bmc). This approach has the advantage that any reduced model at the group level can be estimated efficiently without having to re-estimate the reduced models at the lower level (single-participant levels), and is therefore recommended (Friston et al. 2015). Specifically, a greedy search iteratively prunes connection parameters from the full model until the model evidence starts to decrease, so that the most relevant nested models from the full PEB model are tested (a greedy search is recommended because the model space of all possible nested models is too large to be fully evaluated). Bayesian model averaging of the parameters of the best 256 pruned models is applied and used for group inferences (Zhou et al. 2018), and so determines the winning model empirically. We considered connectivity parameters to be significant when their posterior probability was $P > .95$ (based on model comparisons with and without each parameter). In addition, because the posterior $P > .5$ still make a crucial contribution to the model, we considered them as sub-threshold probabilities. This Bayesian approach to both the first-level connectivity analysis (DCM) and group-level inference (PEB) on the connectivity parameters eschews the multiple-comparisons problem (Friston et al. 2003).

Results

We constructed a model based on a contrast that was present in all studies and showed robust cerebellar and cerebral activation in the mentalizing ROIs (i.e. Social Sequencing > Nonsocial Sequencing). We present the connections across all four studies between and within the cerebellum and cerebrum during social action prediction. Note that we only discuss significant connections with a posterior probability $P > .95$, going from the top left to the top right of Tables 2.

We investigated the common connectivity between cerebellar and cerebral mentalizing areas during the prediction of social action sequences based on various mentalizing processes, including traits, intentions, and preferences across 4 studies (Table 2; Fig. 2). We covaried out differences between individual studies by contrasting the studies against each other (e.g. Study 1 > 2, Study 1 > 3, Study 1 > 4).

Regarding the fixed connections between the cerebellum and cerebrum, we observed a large number of closed loops, specifically, connecting the bilateral Crus 1 with the precuneus and the dmPFC, and the left Crus 1 with the right TPJ, connecting the bilateral Crus 2 with the precuneus and left TPJ, and the right Crus 2 with the dmPFC. We also noted unidirectional connections from the right Crus 1 to the right TPJ, from the left Crus 2 to the dmPFC, from the left TPJ to the right Crus 1 and from the right TPJ to the bilateral Crus 2. Notably, lobule IX only displayed unidirectional connections to the left TPJ and to the dmPFC, and received an incoming connection from the right TPJ. These cerebello-cerebral connections showed a mixed pattern of positive and negative values, although connections with the TPJ tended to be positive.

Within the cerebellum, we also identified a great number of closed loops connecting the left Crus 1 with the right Crus 1 and left Crus 2, connecting the bilateral Crus 2 with the right Crus 1 and lobule IX. Additionally, we noted unidirectional connections

Table 2. Average fixed connections based on the Social Sequencing > Nonsocial Sequencing contrast in all four studies, in units of 1/s (Hz).

from	L Crus1	R Crus1	L Crus2	R Crus2	IX	Precuneus	L TPJ	R TPJ	dmPFC
to	**Fixed connectivity covarying out differences between individual studies (i.e. Study 1 > Study 2, Study 1 > Study 3, Study 1 > Study 4)**								
L Crus1	−0.35**	**0.06****	**−0.03****	0.04**	−0.07**	**0.06****	0.00	**0.03****	**0.09****
R Crus1	**0.07****	−0.35**	**0.14****	**0.10****	0.00	**−0.04****	0.06**	0.01	**−0.07****
L Crus2	**−0.06****	**0.13****	−0.30**	0.01	**0.12****	**−0.02****	**0.07****	0.06**	−0.02*
R Crus2	0.01	**0.12****	0.08**	−0.23**	**0.12****	**−0.09****	**0.10****	0.11**	**−0.05****
IX	0.00	−0.07**	**0.10****	**0.12****	−0.73**	0.00	0.00	−0.05**	0.00
Precuneus	**0.25****	**−0.05****	**0.07****	**−0.05****	0.00	−0.15**	0.08**	**0.17****	**0.13****
L TPJ	0.00	0.02*	**0.04****	**0.06****	0.10**	0.00	−0.33**	**0.10****	0.00
R TPJ	**−0.03****	−0.08**	0.01	0.01	0.01	**0.04****	**0.09****	−0.49**	0.00
dmPFC	**0.25****	**−0.08****	0.08**	**−0.06****	−0.06**	**0.11****	0.04**	0.16**	−0.09**

Note: Cell entries refer to connections from the top row ROIs to the left column ROIs with posterior probabilities;
**$P > .95$ and;
*$P > .50$.
ROIs are ordered from the cerebellum to the cortex. Grey shade denotes self-connections in diagonal cells. Bold denotes significant closed loops with a posterior probability $P > .95$. Differences between studies were controlled for by study-by-study covariates (see text). L = left, R = right, TPJ = temporoparietal junction, mPFC = medial prefrontal cortex.

from the right Crus 1 to lobule IX, from the left Crus 2 to the right Crus 2, and from lobule IX to the left Crus 1. The connections within the cerebellum tended to be largely positive.

Within the cerebrum, we identified closed loops, connecting the precuneus with the right TPJ and dmPFC, and connecting the left and right TPJ. Furthermore, we found unidirectional connections from the left TPJ to the precuneus and from the bilateral TPJ to the dmPFC. The connections within the cerebrum were all positive.

Regarding the modulatory connections, we found no significant changes of connections in the Social versus Nonsocial Sequencing conditions.

Discussion

In the present study, we utilized DCM to explore the connectivity patterns between the cerebellum and cerebrum during the prediction of social actions based on social mentalizing involving traits, intentions, and preferences (Haihambo et al. 2022, 2023a). Our investigation employed an effective connectivity model that exhibited the best fit for the group-level data, which comprised 99 participants from these four studies. Notably, this number is well above the minimum sample size required for a stable DCM, which is approximately 50 (Silchenko et al. 2023).

In alignment with our initial hypothesis, our findings revealed a significant contribution of the cerebellum to social mentalizing through intricate loops involving both interconnections between the cerebellum and cerebrum as well as intra-cerebellar connections. Most of these connections showed clear closed-loop characteristics, which demonstrate that the cerebrum and cerebellum show high levels of sustained neural synchrony between their respective mentalizing areas. Specifically, the cerebello-cerebral loops were particularly pronounced between the cerebellar Crus and cerebral regions encompassing the precuneus, left TPJ and dmPFC. Additionally, cerebellar lobule IX, a region consistently activated across previous studies that served as the basis for our analysis, exhibited unidirectional connectivity with connections terminating in the left TPJ and dmPFC, while receiving connections from the right TPJ.

Social action prediction relies on multiple closed loops between and within cerebellar and cerebral mentalizing areas

As hypothesized, our study unveiled a substantial prevalence of closed-loop connections between cerebellar mentalizing regions in the bilateral Crus and cerebral mentalizing regions, including the precuneus, bilateral TPJ, and dmPFC. The specific cerebellar regions selected for this analysis, namely Crus 1, Crus 2, and lobule IX, have consistently demonstrated robust connectivity within the mentalizing network (Yeo et al. 2011, Buckner et al. 2011, Kawabata et al. 2022). The association of this network with social mentalizing has been supported by prior research examining both neural activation (Van Overwalle et al. 2014, 2015, Haihambo et al. 2022) and effective connectivity (Ma et al., 2022; Van Overwalle et al. 2020b, Metoki et al. 2022, Pu et al. 2022b). In alignment with these earlier investigations, our findings offer additional support for the active communication between posterior cerebellar and cerebral mentalizing regions during social processes, and in particular social prediction.

Intriguingly, connections involving the cerebellum and medial cerebral mentalizing regions (i.e. precuneus and dmPFC) tended to be negative, while those involving the lateral regions (i.e. TPJ) tended to be positive. While the precise implications of positive and negative estimates in DCM, especially with regards to the cerebellum, are not definitively established, positive estimates are often associated with excitatory connections, while negative estimates may indicate inhibitory ones (K. J. Friston et al. 2019). It is worth noting that, consistent with our findings, previous studies have reported positive top-down connections from the TPJ to the posterior cerebellum (Van Overwalle et al. 2020b, Pu et al. 2022b). However, conversely, these previous studies found negative bottom-up connections from the cerebellum to the TPJ, which is in contrast with our positive estimates. One explanation could be that making here and now inferences about traits and predicting future actions based on traits could have differing neural signatures, and therefore engage slightly different connectivity patterns, even though both require mentalizing. To further elucidate this discrepancy, future studies could explore how the temporal aspect of socio-cognitive tasks, such as immediate inferences versus predictive thinking, influences cerebellar connectivity.

An important novelty of our study was the inclusion of cerebellar lobule IX. While prior research has suggested that cerebellar Crus 1, Crus 2, and lobule IX share similar functional connectivity patterns (Xue et al. 2021), our analysis, which specifically incorporated social prediction, yielded distinct differences. Specifically, the majority of connections between the cerebellar Crus and cerebrum exhibit closed-loop patterns, which confirms the hypothesis that there is close reciprocal synchrony between the cerebellum and cerebrum enabling the cerebellar function of social sequence identification for input coming from the cerebrum (Ito 2008, Pisotta and Molinari 2014, Leggio and Molinari 2015, Guell et al. 2018). However, all connections involving lobule IX were unidirectional, projecting from lobule IX to the left TPJ and dmPFC, and from the right TPJ to lobule IX. A possible reason for this difference may be that lobule IX serves a specialized function related to social prediction that is not entirely mirrored by Crus 1 and 2. The TPJ, recognized for its role in social perspective switching and the inference of current mental states from others' actions, and the dmPFC, which is responsible for discerning stable personality traits from social behaviors (Van Overwalle and Baetens 2009, Schurz et al. 2014), potentially receive pivotal information from lobule IX, facilitating precise coordination of social predictive information, which is then projected to the right TPJ. Previous studies have already highlighted structural and functional links between lobule IX and the TPJ during rest (Mars et al. 2012, Chen et al. 2022), and lobule IX has also been structurally connected to prefrontal regional in primates (Kelly and Strick 2003). These findings raise the possibility that lobule IX serves as a critical hub for integrating information essential for future-oriented social cognition. Given that there is only one direct link from the cerebrum (from the right TPJ), most of this information entering lobule IX is likely received from other cerebellar mentalizing areas, primarily through closed loops with Crus 2, which is then transmitted to supporting cerebral mentalizing regions in the dmPFC and TPJ.

Within the cerebellum, we found significant closed loops between the cerebellar lobule IX and Crus 2, which supports the above assumption that Crus 2 may inform lobule IX about critical information for social prediction. Both areas have been consistently activated in social prediction studies (Haihambo et al. 2022, 2023a, 2023b). Bilateral Crus 2 has been strongly implicated in social processing during mentalizing (Van Overwalle et al. 2020a), while lobule IX is associated with future-oriented thinking and abstraction (Habas et al. 2009, Van Overwalle et al. 2014, 2015, Guell et al. 2018). We further unveiled bidirectional connections

between the bilateral cerebellar Crus regions, a pattern that, while consistent with previous studies conducted within our lab (Ma et al., 2022; Van Overwalle et al. 2020b, Pu et al. 2022b), appears to be more extensive in the present study. Notably, all closed loop connections within the cerebellum exhibited positive values, except for those between the left Crus 1 and left Crus 2. This heightened connectivity could potentially indicate that future-oriented thinking relies on a more intensive information exchange among posterior cerebellar areas.

Within the cerebrum, we identified closed loops involving the precuneus, right TPJ, and dmPFC, as well as between the left and right TPJ, indicating reciprocal information exchange and underscoring the pivotal roles of these regions in jointly processing and interpreting social cues. Furthermore, unidirectional connections, such as those from the bilateral TPJ to the dmPFC, suggest a hierarchical flow of information within the cerebral mentalizing network. These directional connections imply sequential processing of social information, where the bilateral TPJ integrates socially oriented information, which is then transmitted to the dmPFC enabling further abstract inferences, such as traits. Importantly, all these connections were estimated to be positive. Together these results contribute existing knowledge on the relatively stable intrinsic connectivity of cerebral mentalizing areas in both resting-state functional connectivity (Yeo et al. 2011, Raichle 2015, Razi et al. 2015, Silchenko et al. 2023) and social mentalizing-driven effective connectivity (Ma et al., 2022; Van Overwalle et al. 2019b, 2020b, Wang et al. 2021, Pu et al. 2022b).

No modulation in connections for trait, intention, and preference prediction

Our study revealed an absence of modulatory connections between social and nonsocial conditions. This observation suggests that neural connectivity patterns remain remarkably stable, irrespective of the specific task demands, underscoring a consistent functional state within these brain regions during social prediction based on mentalizing inferences. Consistent with this, in the original studies, we observed significant differences in activation in cerebellar and cerebral mentalizing areas when comparing social versus nonsocial conditions. However, these activations did not correspond to changes in connectivity within our ROIs. This may indicate that while social information processing involves distinct localized activity within these regions, the information exchange through connectivity is similar across conditions. This intriguing finding aligns with previous DCM research, which similarly reported minimal modulation during tasks involving social mentalizing (Van Overwalle et al. 2019b, 2020b, Pu et al. 2022b, Ma et al. 2023a). One explanation for this phenomenon lies in the innate social nature of humans. It is plausible that humans have evolved to maintain a continuous readiness for social stimuli, a predisposition that persists even in situations devoid of overtly social characteristics, such as nonsocial trials. A related explanation is the fact that social and nonsocial trials were presented randomly during the experiments, which may have encouraged a constant social-oriented mindset. Nonetheless, this result raises speculative questions about the inherent resistance to modulation in high-level mental reasoning processes encompassing both social and nonsocial facets, when exposed to diverse contextual conditions.

Conclusion

Our findings confirm the existence of robust closed loops between the posterior cerebellar Crus regions and cerebral mentalizing areas, including the precuneus, TPJ, dmPFC during social prediction. Additionally, we unveil previously unexplored unidirectional loops between lobule IX and the cerebrum.

Author contributions

N.H. and F.V.O. conceived the study, N.H. conducted the experiment and conducted the data analyses based in part on scripts written by F.V.O. N.H. and F.V.O. interpreted the results, N.H. drafted the manuscript, F.V.O. edited the manuscript, and all authors reviewed the manuscript.

Conflict of interest: None declared.

Funding

This work was supported by the Strategic Research Program SRP57 from the Vrije Universiteit Brussel awarded to F.V.O.

Data availability

All requested (pseudonymized or anonymous) data are available upon request, excluding data that allow identifying individual participants. All manuals and code for processing the data are also available together with the data.

References

Addis DR, Pan L, Vu MA *et al.* Constructive episodic simulation of the future and the past: distinct subsystems of a core brain network mediate imagining and remembering. *Neuropsychologia* 2009;**47**:2222–38. https://doi.org/10.1016/j.neuropsychologia.2008.10.026

Addis DR, Wong AT, Schacter DL. Remembering the past and imagining the future: Common and distinct neural substrates during event construction and elaboration. *Neuropsychologia* 2007;**45**:1363–77. https://doi.org/10.1016/j.neuropsychologia.2006.10.016

Blakemore SJ, Frith CD, Wolpert DM. The cerebellum is involved in predicting the sensory consequences of action. *NeuroReport* 2001;**12**:1879–84. https://doi.org/10.1097/00001756-200107030-00023

Buckner R, Krienen F, Castellanos A *et al.* The organization of the human cerebellum estimated by intrinsic functional connectivity. *J Neurophysiol* 2011;**106**:2322–45. https://doi.org/10.1152/jn.00339.2011

Chen Z, Zhang R, Huo H *et al.* Functional connectome of human cerebellum. *NeuroImage* 2022;**251**:119015. https://doi.org/10.1016/j.neuroimage.2022.119015

Cusack R, Papadakis N. New robust 3-D phase unwrapping algorithms: application to magnetic field mapping and undistorting echoplanar images. *NeuroImage* 2002;**16**:754–64. https://doi.org/10.1006/nimg.2002.1092

Friston KJ, Harrison L, Penny W. Dynamic causal modelling. *NeuroImage* 2003;**19**:1273–302. https://doi.org/10.1016/S1053-8119(03)00202-7

Friston KJ, Litvak V, Oswal A *et al.* Bayesian model reduction and empirical Bayes for group (DCM) studies. *NeuroImage* 2016;**128**:413–31. https://doi.org/10.1016/j.neuroimage.2015.11.015

Friston KJ, Preller KH, Mathys C *et al.* Dynamic causal modelling revisited. *NeuroImage* 2019;**199**:730–44. https://doi.org/10.1016/j.neuroimage.2017.02.045

Friston K, Zeidman P, Litvak V. Empirical Bayes for DCM: a group inversion scheme. *Front Syst Neurosci* 2015;**9**:164. https://doi.org/10.3389/fnsys.2015.00164

Frith CD, Frith U. How we predict what other people are going to do. *Brain Res* 2006;**1079**:36–46. https://doi.org/10.1016/j.brainres.2005.12.126

Guell X, Schmahmann JD, Gabrieli JDE *et al*. Functional gradients of the cerebellum. *ELife* 2018;**7**:e36652. https://doi.org/10.7554/eLife.36652

Habas C, Kamdar N, Nguyen D *et al*. Distinct cerebellar contributions to intrinsic connectivity networks. *J Neurosci* 2009;**29**:8586–94. https://doi.org/10.1523/JNEUROSCI.1868-09.2009

Haihambo N, Ma Q, Baeken C *et al*. Social thinking is for doing: the posterior cerebellum supports predictions of social actions based on personality traits. *Soc Cognit Affect Neurosci* 2022;**17**:241–51. https://doi.org/10.1093/scan/nsab087

Haihambo N, Ma Q, Baetens K *et al*. Two is company: the posterior cerebellum and sequencing for pairs versus individuals during social preference prediction. *Cognit Affective Behav Neurosci* 2023a;**23**:1482–99. https://doi.org/10.3758/s13415-023-01127-y

Haihambo N, Ma Q, Baetens K *et al*. To do or not to do: the cerebellum and neocortex contribute to predicting sequences of social intentions. *Cognit Affective Behav Neurosci* 2023b;**23**:323–39. https://doi.org/10.3758/s13415-023-01071-x

Heleven E, van Dun K, Van Overwalle F. The posterior cerebellum is involved in constructing social action sequences: an fMRI study. *Sci Rep* 2019;**9**:11110. https://doi.org/10.1038/s41598-019-46962-7

Hillebrandt H, Friston KJ, Blakemore SJ. Effective connectivity during animacy perception - dynamic causal modelling of Human Connectome Project data. *Sci Rep* 2014;**4**:1–9. https://doi.org/10.1038/srep06240

Ito M. Control of mental activities by internal models in the cerebellum. *Nat Rev Neurosci* 2008;**9**:304–13. https://doi.org/10.1038/nrn2332

Kawabata K, Bagarinao E, Watanabe H *et al*. Functional connector hubs in the cerebellum. *NeuroImage* 2022;**257**:119263. https://doi.org/10.1016/j.neuroimage.2022.119263

Kelly RM, Strick PL. Cerebellar loops with motor cortex and prefrontal cortex of a nonhuman primate. *J Neurosci* 2003;**23**:8432–44. https://doi.org/10.1523/jneurosci.23-23-08432.2003

Leggio M, Molinari M. Cerebellar sequencing: a trick for predicting the future. *Cerebellum* 2015;**14**:35–38. https://doi.org/10.1007/s12311-014-0616-x

Li M, Ma Q, Baetens K *et al*. Social cerebellum in goal-directed navigation. *Socl Neurosci* 2021;**16**:467–85. https://doi.org/10.1080/17470919.2021.1970017

Li M, Pu M, Baetens K *et al*. Mind your step: social cerebellum in interactive navigation. *Soc Cognit Affect Neurosci* 2023;**18**:nsac047. https://doi.org/10.1093/scan/nsac047

Ma Q, Pu M, Haihambo N *et al*. Effective cerebello–cerebral connectivity during implicit and explicit social belief sequence learning using dynamic causal modeling. *Soc Cognit Affect Neurosci* 2023a;**18**. https://doi.org/10.1093/scan/nsac044

Ma Q, Pu M, Haihambo NP *et al*. The posterior cerebellum and temporoparietal junction support explicit learning of social belief sequences. *Cognit Affect Behav Neurosci* 2021a;**21**:970–92. https://doi.org/10.3758/s13415-021-00966-x

Ma Q, Pu M, Heleven E *et al*. The posterior cerebellum supports implicit learning of social belief sequences. *Cognit Affective Behav Neurosci* 2021b;**21**:970–92. https://doi.org/10.3758/s13415-021-00910-z

Mars RB, Sallet J, Schüffelgen U *et al*. Connectivity-based subdivisions of the human right "temporoparietal junction area": Evidence for different areas participating in different cortical networks. *Cereb Cortex* 2012;**22**:1894–903. https://doi.org/10.1093/cercor/bhr268

Metoki A, Wang Y, Olson IRR. The social cerebellum: a large-scale investigation of functional and structural specificity and connectivity. *Cereb Cortex* 2022;**32**:987–1003. https://doi.org/10.1093/cercor/bhab260

Molenberghs P, Trautwein FM, Böckler A *et al*. Neural correlates of metacognitive ability and of feeling confident: a large-scale fMRI study. *Soc Cognit Affect Neurosci* 2016;**11**:1942–51. https://doi.org/10.1093/scan/nsw093

Pisotta I, Molinari M. Cerebellar contribution to feedforward control of locomotion. *Front Human Neurosci* 2014;**8**:1–5. https://doi.org/10.3389/fnhum.2014.00475

Pu M, Heleven E, Delplanque J *et al*. The posterior cerebellum supports the explicit sequence learning linked to trait attribution. *Cognit Affect Behav Neurosci* 2020;**20**:798–815. https://doi.org/10.3758/s13415-020-00803-7

Pu M, Ma Q, Haihambo N *et al*. Dynamic causal modeling of cerebello-cerebral connectivity when sequencing trait-implying actions. *Cereb Cortex* 2022b;**2020**:1–16. https://doi.org/10.1093/cercor/bhac510

Raichle ME. The brain's default mode network. *Annu Rev Neurosci* 2015;**38**:433–47. https://doi.org/10.1146/annurev-neuro-071013-014030

Razi A, Kahan J, Rees G *et al*. Construct validation of a DCM for resting state fMRI. *NeuroImage* 2015;**106**:1–14. https://doi.org/10.1016/j.neuroimage.2014.11.027

Schurz M, Radua J, Aichhorn M *et al*. Fractionating theory of mind: a meta-analysis of functional brain imaging studies. *Neurosci Biobehav Rev* 2014;**42**:9–34. https://doi.org/10.1016/j.neubiorev.2014.01.009

Silchenko AN, Hoffstaedter F, and Eickhoff SB. Impact of sample size and regression of tissue-specific signals on effective connectivity within the core default mode network. *Human Brain Mapp* **44** 2023:1–13. https://doi.org/10.1002/hbm.26481

Sokolov AA, Miall RC, Ivry RB. The cerebellum: adaptive prediction for movement and cognition. *Trends Cognit Sci* 2017;**21**:313–32. https://doi.org/10.1016/j.tics.2017.02.005

Van Overwalle F. Social cognition and the brain: a meta-analysis. *Human Brain Mapp* 2009;**30**:829–58. https://doi.org/10.1002/hbm.20547

Van Overwalle F, Baetens K. Understanding others' actions and goals by mirror and mentalizing systems: a meta-analysis. *NeuroImage* 2009;**48**:564–84. https://doi.org/10.1016/j.neuroimage.2009.06.009

Van Overwalle F, Baetens K, Mariën P *et al*. Social cognition and the cerebellum: a meta-analysis of over 350 fMRI studies. *NeuroImage* 2014;**86**:554–72. https://doi.org/10.1016/j.neuroimage.2013.09.033

Van Overwalle F, D'aes T, Mariën P. Social cognition and the cerebellum: a meta-analytic connectivity analysis. *Human Brain Mapp* 2015;**36**:5137–54. https://doi.org/10.1002/hbm.23002

Van Overwalle F, Ma Q, Heleven E. The posterior crus II cerebellum is specialized for social mentalizing and emotional self-experiences: a meta-analysis. *Soc Cognit Affect Neurosci* 2020a;**15**:905–28. https://doi.org/10.1093/scan/nsaa124

Van Overwalle F, Manto M, Leggio M *et al*. The sequencing process generated by the cerebellum crucially contributes to social interactions. *Med Hypotheses* 2019a;**128**:33–42. https://doi.org/10.1016/j.mehy.2019.05.014

Van Overwalle F, Van de Steen F, Mariën P. Dynamic causal modeling of the effective connectivity between the cerebrum and cerebellum in social mentalizing across five studies. *Cognit Affect Behav Neurosci* 2019b;**19**:211–23. https://doi.org/10.3758/s13415-018-00659-y

Van Overwalle F, Van de Steen F, van Dun K *et al*. Connectivity between the cerebrum and cerebellum during social and non-social sequencing using dynamic causal modelling. *NeuroImage* 2020b;**206**:116326. https://doi.org/10.1016/j.neuroimage.2019.116326

Wang Y, Metoki A, Xia Y *et al*. A large-scale structural and functional connectome of social mentalizing. *NeuroImage* 2021;**236**:118115. https://doi.org/10.1016/j.neuroimage.2021.118115

Xue A, Kong R, Yang Q *et al*. The detailed organization of the human cerebellum estimated by intrinsic functional connectivity within the individual. *J Neurophysiol* 2021;**125**:358–84. https://doi.org/10.1152/jn.00561.2020

Yeo BTT, Krienen FM, Sepulcre J *et al*. The organization of the human cerebral cortex estimated by intrinsic functional connectivity. *J Neurophysiol* 2011;**106**:1125–65. https://doi.org/10.1152/jn.00338.2011

Zhou Y, Liang M, Tian L *et al*. Functional disintegration in paranoid schizophrenia using resting-state fMRI. *Schizophr Res* 2007;**97**:194–205. https://doi.org/10.1016/j.schres.2007.05.029

Zhou Y, Zeidman P, Wu S *et al*. Altered intrinsic and extrinsic connectivity in schizophrenia. *NeuroImage Clin* 2018;**17**:704–16. https://doi.org/10.1016/j.nicl.2017.12.006

Social Cognitive and Affective Neuroscience, 2025, 20(1), nsaf019, DOI: https://doi.org/10.1093/scan/nsaf019, Advance Access Publication Date: 15 February 2025, Original Research – Neuroscience
Received: 24 October 2023; Revised: 30 January 2025; Accepted: 13 February 2025